CHEMISTRY
A EUROPEAN JOURNAL

COMMUNICATION

DOI: 10.1002/chem.201300009

Carbon Nano-Onions and Biocompatible Polymers for Flavonoid Incorporation

Marta E. Plonska-Brzezinska,*[a] Diana M. Brus,[a] Joanna Breczko,[a] and Luis Echegoyen*[b]

In recent years, nanotechnology, which is defined as the creation and control of the properties of nanometric-scale objects, has been playing an increasingly significant role in medicine, material engineering, and pharmacology. The potential applications of carbon nanostructures in biotechnology and nanomedicine is particularly noteworthy.[1] Carbon nanotubes (CNTs) are useful materials in a variety of biomedical applications, particularly in biosensing and optical imaging, and also in novel therapeutic strategies.[2] Using CNTs as signal transducers in biosensors has resulted in improved detection limits and signal amplification because they possess multiple biorecognition elements attached to a single tube.[3,2a] Despite the progress, there are still many challenges related to issues of the reproducible synthesis of CNTs with well-defined structures and physicochemical properties. Some of these problems include the prevention of nanotube aggregation during electrode modification, the effective separation of semiconducting and conducting CNTs, and separation of nanotubes with uniform lengths. It has been previously observed that the reactivity of fullerene-like structures decreases with increasing size owing to a decrease of the curvature of the molecule.[4] While the various forms of CNTs are chemically inert, their ends and sidewalls can be functionalized by a variety of chemical groups. Small carbon nano-onions (CNOs) are potentially better systems for some of these applications, because they show higher reactivity and solubility in many solvents. Various reactions have been reported for CNOs using strategies such as oxidation of defects,[5] fluorination,[6] radical addition,[7] 1,3-dipolar cycloaddition,[8] or polymerization.[9] Our studies have shown that small carbon nano-onions can also be used as components of conductive nanocomposites, increasing the specific capacity of the layers on the surface of the electrodes.[10–13] Nanostructures with conductive polymers (polyaniline)[10–12] and polyelectrolytes[13] have also been prepared and used in the detection of neurohormones, such as dopamine.[14] In addition, the good biocompatibility and low cytotoxicity of CNOs are also very promising. Studies of normal cells (human skin fibroblasts), conducted with the MTT method using CNOs, confirm the low toxicity and good biocompatibility of these carbon nanostructures over a wide range of concentrations.[15] Additionally, it is possible to modify the surfaces of CNOs with biomolecules without loss of their activity. We have worked specifically with the avidin–biotin model system.

Polyphenolic compounds, such as flavonoids, exhibit protective effects on humans, for instance, in the prevention of cardiovascular diseases.[16] It has been shown that flavonoids could be successfully applied in traditional medicine for the treatment of inflammations, wounds, certain forms of cancer, infections, diarrhea, diabetes mellitus, and other ailments.[17,18] Polyphenolic compounds interact with proteins mainly by hydrophobic/ionic interactions. Quercetin (Q, 3,3′,4′,5,7-pentahydroxyflavone; Scheme 1) is a polyphenolic

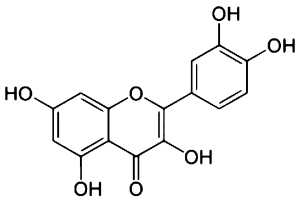

Scheme 1. Structure of quercitin.

flavonoid that is widely distributed in nature. It is derived from quercetum (oak trees) and has anti-inflammatory properties[19] as a calcineurin inhibitor, similar to cyclosporin A. Owing to its mast cell inhibitory properties, it could be effective in the treatment of fibromyalgia.[20] This flavonoid is contraindicated with some antibiotics. It may interact with fluoroquinolones and competitively bind to bacterial DNA gyrase.[21]

It is necessary to target polyphenolic molecules to selected locations in the organism. To accomplish this goal, nanostructured surfaces with well-defined physicochemical properties need to be prepared to target specific locations. Carbon nano-onions are nanostructures which are easily

[a] Dr. M. E. Plonska-Brzezinska, D. M. Brus, J. Breczko
Institute of Chemistry, University of Bialystok
Hurtowa 1, 15-399 Bialystok (Poland)
Fax: (+48) 85-7470113
E-mail: mplonska@uwb.edu.pl

[b] Prof. L. Echegoyen
Department of Chemistry, University of Texas at El Paso
500 W. University Ave., El Paso, TX 79968 (USA)
Fax: (+1) 915-7478807
E-mail: echegoyen@utep.edu

Supporting information for this article is available on the WWW under http://dx.doi.org/10.1002/chem.201300009.

functionalized. Additionally, their average sizes (5–6 nm) enables their use in both in vitro and in vivo studies.

The number of articles involving CNOs with polymer functionalization is still very sparse.[10,22] Poly(4-vinylpyridine-*co*-styrene)[23] (PVPS) and poly(ethylene glycol)[24] (PEG) have been frequently used for solubilization of carbon nanostructures in non-polar or polar media. Attaching hydrophilic or hydrophobic chains to synthesize soluble derivatives of CNOs have been reported. The non-covalent functionalization of carbon nano-onions with a poly(ethylene glycol)/polysorbate 20 (PEG/P20) mixture or with PVPS generates charged CNO surfaces for further functionalization with other moieties. The procedure for functionalization of oxidized CNOs (ox-CNOs) with PEG/P20 or pristine CNOs with PVPS polymers is depicted in Scheme 2. Non-modified CNOs tend to aggregate because of strong van der Waals interactions between them. Therefore, the first step in the functionalization with PEG/P20 (Scheme 2a), involved oxidation of the carbon nanoparticles, to increase their dispersion in a DMF/EtOH mixture. Next, the PEG/P20 polymer layer was formed on the ox-CNO surface. The modification with PVPS provided the matrix to incorporate the thiol derivatives (Scheme 2b): 3-mercaptopropionic (MPA) or 2-mercapto-4-methyl-5-thiazoleacetic (MMTA) acids.[25] The C=C groups in the CNO/PVPS competitively reacted with the SH-containing compounds, and after 48 h at 30 °C, a PVPS matrix having carboxyl pendant groups was obtained. The well-dispersed CNO/PEG/P20 and CNO/PVPS composites modified with thiol derivatives were used for the electrostatic immobilization of the polyphenolic compounds.

The functionalization of the carbon nanostructures with the polymer network was confirmed by TEM studies at high magnification. The thickness and uniformity of the polymer layer on the carbon nanostructures depends on the kind of polymer used (see arrows in Figure 1). However, the functionalization of ox-CNOs with the PEG/P20 mixture leads to the formation of non-uniform layers, and these modifiers ensure sufficient dispersion in polar solvents (Figures 1a, 2d). Carbon nano-onion structures with homogeneous polymer layers were obtained by the PVPS modification and can be clearly seen using TEM (Figure 1b). The size is indicative of the formation of a relatively thin and uniform layer with about 1 nm thickness. Adsorption of the PEG/P20 and PVPS polymers on the ox-CNO or CNO surfaces, respectively, resulted in improved dispersion and enabled further modification of the CNO/PVPS with thiols. CNO/PVPS modification (Figure 1b, inset and Figure 2a) with thiol derivatives: MMTA (Figure 2b) and MPA (Fig-

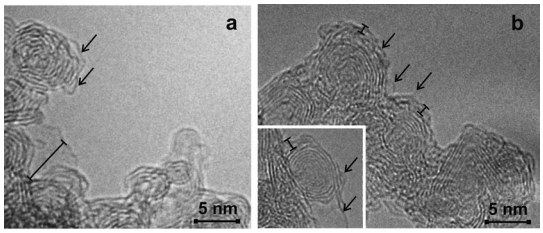

Figure 1. HR-TEM images of a) CNO/PEG-P20 and b) CNO/PVPS-MPA. Inset: CNO/PVPS.

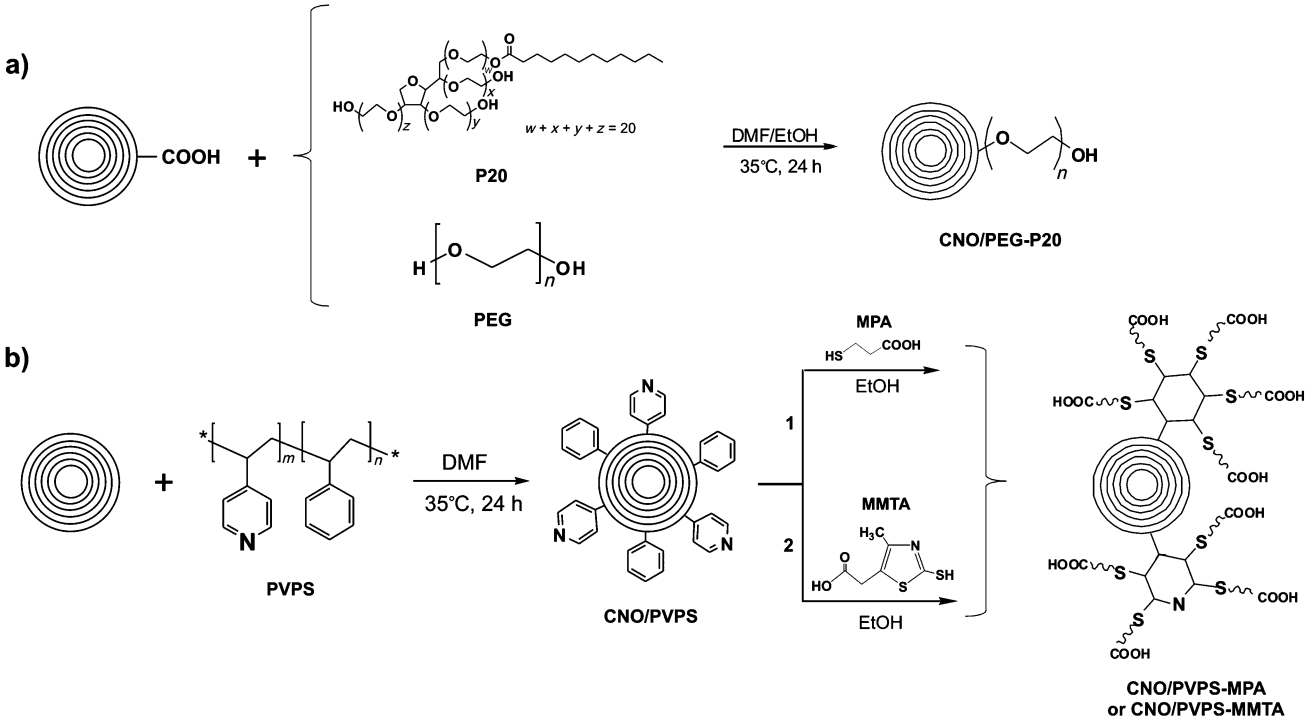

Scheme 2. Functionalization of a) ox-CNOs by PEG/P20 and b) CNOs by PVPS with thiol molecules.

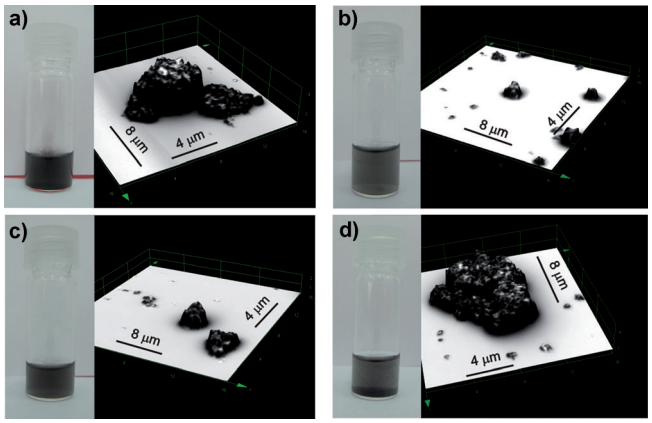

Figure 2. Confocal microscope images of the slide covered with a) CNO/PVPS, b) CNOs/PVPS-MMTA, c) CNO/PVPS-MPA, and d) CNO/PEG/P20. An solution/suspension of functionalized CNOs in ethanol is also shown.

ures 1b, 2c), respectively, increased their solubility in polar solvents.

The results of SEM studies of a gold foil covered with CNO, CNO/PEG/P20, CNO/PVPS-MPA, or CNO/PVPS-MMTA composites are shown in Figure 3. The micrographs

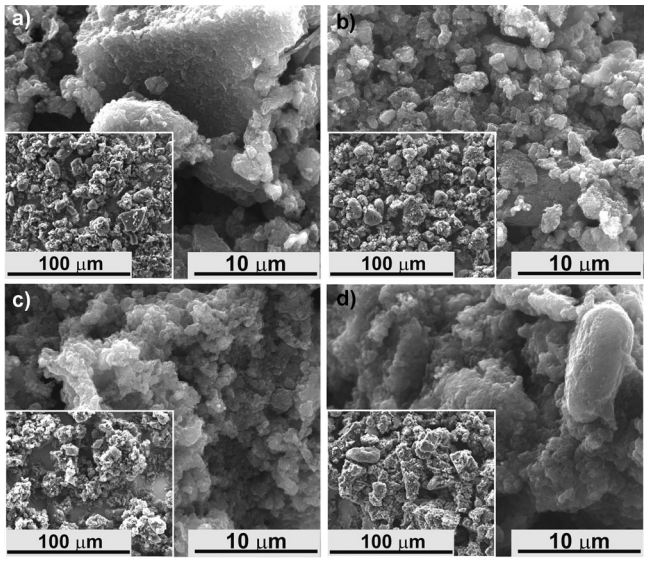

Figure 3. SEM images of the Au foil covered with a) CNO/PVPS, b) CNOs/PVPS-MMTA, c) CNO/PVPS-MPA, and d) CNO/PEG/P20.

(Figure 3b–d) clearly reveal that the polymer wrappings significantly increase the dispersion of the carbon nanostructures in the appropriate solvents (Figure 2, inset). A comparison of Figure 3b with 3c,d, and of Figure 2a with 2b,c (confocal microscopy), clearly shows enhanced dispersion of the CNO/PVPS composites after functionalization with thiol derivatives MMTA and MPA, especially in polar solvents, including water (Figure 2b,c).

FTIR spectra of the CNO/PEG/P20 and CNO/PVPS composites (Supporting Information, Figure S1) and pristine

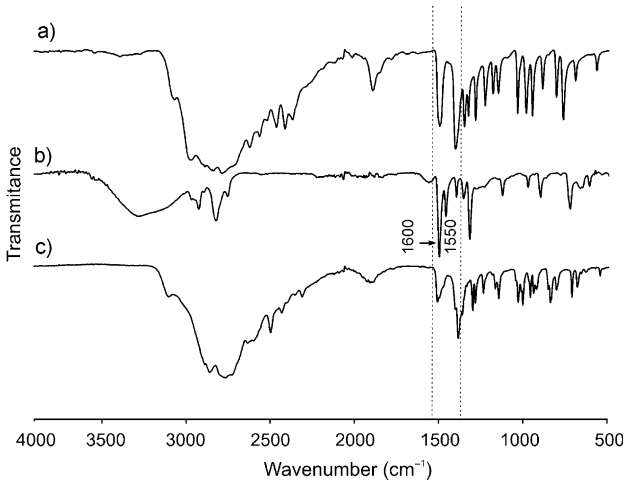

Figure 4. FTIR spectra in the range 4000-500 cm^{-1} of a) MPA, b) PVPS, and c) PVPS-MPA. The spectra were recorded at room temperature under a N_2 atmosphere.

components PVPS, MPA, and PVPS-MPA (Figure 4) were obtained to determine the presence of polymer and thiol derivatives in the composite structures. FTIR was used to analyse the changes in the surface chemical bonding and structure, within the frequency range 4000–100 cm^{-1}. The FTIR spectra of the CNO/PVPS composite is dominated by the absorptions of polystyrene (Supporting Information, Figure S1a).[26] The vibrational behaviour of vinylpyridine is similar to that of polystyrene, because of the polyvinyl chains. Earlier IR studies suggested that the absorption modes at about 1500 cm^{-1} and 1600 cm^{-1} are associated with aromatic ring stretching.[27] The bands at 1585 and 1540 cm^{-1} were attributed to the stretching modes of the pyridine ring, and are associated with the C=N and C=C stretching vibrations of the rings (Supporting Information, Figure S1a).[28] The band at 1405 cm^{-1} is assigned to the PVPS block. The overlapped peaks in the range between 1150 and 900 cm^{-1} are attributed to the in-plane bending vibrations of aromatic C–H.[29] Therefore the peaks at 820 and 698 cm^{-1} are attributed to the out-of-plane bending vibrations of C–H bonds in the aromatic rings. To analyse the contribution from the inner carbon nano-onion core to the FTIR spectra, model polymers were prepared and analyzed. The IR spectra of the functionalized PVPS copolymer with MPA are presented in Figure 4. The feature that identifies carboxylic acids is a broad absorption band, which extends from 3300 to 2500 cm^{-1}.[30] The broadening of this band is due to intermolecular hydrogen bonds, which weaken the O–H bonds.[31] This broad band was observed in pristine 3-mercaptopropionic acid (Figure 4a) as well as for the PVPS-MPA copolymer (Figure 4c). The vibrational modes at 1550 and 1600 (Figure 4b), are associated with the C=N and C=C bonds of the pyridine and benzene rings. A decrease of the intensity of these peaks for the modified PVPS-MPA copolymer is due to saturation of the double bonds and is indicative of PVPS functionalization with the thiol molecules (Figure 4c).

The FTIR measurements were also performed to provide evidence of the attached PEG/P20 mixture to the carbon nanostructures. A peak at 1740 cm^{-1} corresponds to the C=O stretching mode of the carbonyl groups of the P20 chain (Supporting Information Figure S1b).[29] The peaks at 1280 and 1220 cm^{-1} are attributed to primary and secondary O–H in-plane bending.[32] Therefore the peak at about 720 cm^{-1} corresponds to the O–H out-of-plane bending. The CNO/PEG/P20 spectra show peaks at 1160, 1110, and 1070 cm^{-1} that correspond to the C–O stretch vibrations of the PEG and P20 chains.[29] Methyl bands at 1510, 1450 and about 720 cm^{-1} are indicative of the long-chain aliphatic structures of the polymers.[33] More peaks are observed between 2807 and 2970 cm^{-1} from the symmetric and unsymmetric C–H stretching of the PEG and P20 chains. Some additional C–C vibrations from polymeric chains occur below 1300 and 700 cm^{-1}. It is clear that PEG and P20 were incorporated in the composite structures.

Raman spectroscopic analyses of the two G and D lines were used to characterize the carbon samples. The strongest features for the CNO/PVPS and CNO/PVPS-MPA composites (Supporting Information, Figures S2c,d, S3) are observed at about 1340 (D line) and 1580 cm^{-1} (G line). The band at 1340 cm^{-1} is related to the disorder of the graphite lattice.[34] For our compound, closer examination of the feature observed at 1580 cm^{-1}, assigned to the E_{2g} species of the infinite crystal, shows[30] that it is composed of two components (Supporting Information, Figure S3). In addition to the G band (ca. 1580 cm^{-1}), another at about 1618 cm^{-1} (D′ band) is observed. Besides the strong D and G features observed in the Raman spectra of CNOs/PVPS, an additional band is observed at about 2680 cm^{-1}, which is assigned to overtone scattering (1340 $cm^{-1} \times 2$). The bands observed between 1063 and 1595 cm^{-1} indicate the presence of two carbon–nitrogen bonds (Supporting Information, Figure S2b).[35] The bands at 1063 and 1200 cm^{-1} can be associated with the ν(C–N) modes, and at 1595 cm^{-1} with the ν(C=N) modes of the pyridine rings, respectively. The C–H bending modes occur at 665, 990, and 3045 cm^{-1} and are due to the aromaticity of the pyridine and benzene rings in the PVPS chain, whereas the weak bands from 2850 to 2950 cm^{-1} can be associated with the alkyl C–H stretching modes of the polymer. These spectral data provide evidence for the presence of the PVPS copolymer on the CNO surfaces and are consistent with the structure depicted in Scheme 1.

The non-covalent modification with flavonoid compounds was achieved by sonication of aqueous dispersions of polymer-terminated CNO derivatives (CNOs/PEG/P20, CNO/PVPS-MPA or CNOs/PVPS-MMTA) with quercetin. Previous studies showed that amylose or branched amylopectin form supramolecular complexes with SWNTs in aqueous solution.[32] Such modification would lead to the creation of hydrogen-bonding polymer-terminated carbon nanostructures/polyphenolic complexes.

The interaction between the carbon nano-onion composites and quercetin was studied by fluorescence spectroscopy. It is generally known that quercetin is fluorescent in many solvents.[33a,36] The interesting aspect of flavonoids relates to their unusual fluorescence emission properties, which are extremely sensitive to the surrounding medium (for example, polarity, hydrogen bonding effects, pH, or temperature).[33] The fluorescence measurements were performed in non-aqueous solutions. Excitation and emission spectra for the supramolecular complexes of CNO composites with Q in dimethyl sulfoxide solution are shown in Figure 5 and the Supporting Information, Figure S4. Two interesting observations were made: that the modification of PVPS with the thiol derivatives, MMTA or MPA, lead to decreased emission of the CNO composites, which is due to changes of the hybridization of the carbon atoms from sp^2 to sp^3 in the pyridine or benzene rings of the polymer. PEG and the CNOs/PEG composites showed very low fluores-

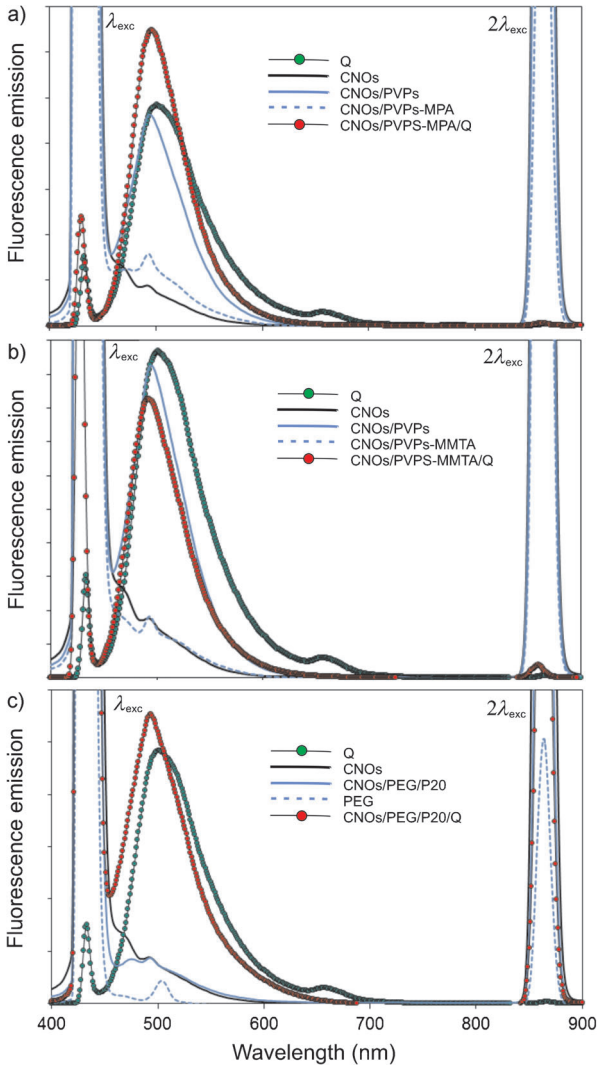

Figure 5. Fluorescence emission spectra of quercetin, carbon nano-onions, and their composites with: a) PVPS-MPA, b) PVPS-MMTA, and c) PEG/P20 (excitation and emission bandwidths: 5 nm).

cence emission under these experimental conditions (Figure 5c). The emission spectrum of quercetin in dimethyl sulfoxide upon excitation at 430 nm exhibits a maximum around 505 nm (Figure 5), the intensity of which is proportional to the concentration of the different composites including modified CNOs and Q in solution (Supporting Information, Figure S4). Upon further modification of the CNO composites with flavonoids and the subsequent creation of hydrogen bonds, the emission wavelength of the incorporated Q exhibited a bathochromic shift of about 15 nm from the original band for the CNOs/PVPS derivatives and the CNOs/PEG composites. This observation is consistent with previously observed protein and quercetin complexes, where intermolecular C−OH···O=C bonds lead to shifts of the fluorescence emission of Q.[36b]

In summary, combining the non-covalent functionalization approach with the use of PVPS or PEG/P20 has thus provided a facile and easy way to modify CNOs. PVPS polymers confer good solubility on the CNOs and create a matrix for further functionalization with thiol derivatives. The incorporated hydrophilic CNO composites prepared successfully incorporated flavonoids, which are promising for biosensing and drug targeting applications.

Experimental Section

All of the chemicals and solvents used are commercially available and were used without further purification. The films were imaged by secondary-electron SEM with the use of a INSPECT S50 Scanning Electron Microscope from FEI. The accelerating voltage of the electron beam was 15 keV and the working distance was 10 mm. Transmission electron microscopy analyses were performed with a FEI instrument operated at 200 kV. The materials were sonicated in ethanol for 30 min and deposited on copper grids. A 3D microscope LEXT OLS4000 with a 405 nm laser and confocal optical system from Olympus was used for surface roughness measurements. The fluorescence spectra were recorded on a Hitachi F-7000 fluorescence spectrophotometer: excitation bandwidths 5.0 nm, emission bandwidths 5.0 nm, scan speed 1200 nm min^{-1}, PMT voltage 400 V. FTIR spectra were recorded in the range between 4000 and 100 cm^{-1} with a Nicolet 6700 Thermo Scientific spectrometer at room temperature and N_2 atmosphere. The spectra were collected with a resolution of 4 cm^{-1}. All the spectra were corrected with conventional software in order to cancel the variation of the analyzed thickness with the wavelength. The room-temperature Raman spectra at wavelengths between 100 and 3500 cm^{-1} were investigated using a Renishaw in Via Reflex spectrometer. To avoid sample overheating, the power of the laser beam was reduced to about 3 mW. The position of the Raman peaks was calibrated using a Si thin film as an external standard. The spectral resolution of the Raman spectra was 2 cm^{-1}.

Synthesis of CNO composites: Small CNOs were obtained by annealing nanodiamond powder (Molto, 5 nm average particle size) under a positive pressure of helium at 1650 °C for 1 h.[37] After separation and purification, CNOs were heated at 200 °C to remove the amorphous carbon residue from the CNO surface. High-resolution transmission electron microscopy images of the CNOs have been reported elsewhere.[5]

Functionalization of CNOs with PEG/P20: 20 mg of crude 6–8 shell CNOs were dispersed by ultrasonication for 30 min and refluxed for 8 h in 3 M nitric acid. The mixture was then centrifuged for 10 min, and the black powder collected in the bottom of the test tube was washed several times with deionized water and dried overnight in a vacuum oven (T = 100 °C). The black powder was mixed with 500 μL of poly(ethylene glycol) (PEG 1500 30% solution in H_2O, referred in preceding text as PEG) and 20 μL of Polysorbate 20 (P20) in a DMF/EtOH solution mixture at 35 °C for 24 h. Next, unreacted poly(ethylene glycol) was removed by dialyzing the mixture using a spectra pore dialysis membrane (MWCO 15000).

Functionalization of CNOs with PVPS and MPA or MMTA: 20 mg of crude 6–8 shell CNOs were dispersed with 10 mg of poly(4-vinylpyridine-*co*-styrene) (PVPS) by ultrasonication in a DMF solution at 35 °C for 24 h. Next, 10 mg of the CNO/PVPS composite was dissolved in EtOH solution (5 mL), and then slowly added to 7.2 mg of 3-mercaptopropionic acid (MPA) or 8.4 mg 2-mercapto-4-methyl-5-thiazoleacetic acid (MMTA) in ethanol (4 mL).[38] After standing at 30 °C for 48 h, the solution was dialysed against running deionized water. The CNO composites was added into DMF solution with 2 mg of quercetin. The solution was sonicated for 30 min to form a homogenuos solution. The solution was then heated at 180 °C for 3 h in an autoclave to form CNO/PVPS-MPA/Q or CNO/PVPS-MMTA/Q.

Acknowledgements

The authors thank Agustin Molina-Ontoria (Texas University at El Paso, USA) for CNO synthesis. We gratefully acknowledge the financial support of the NCN, Poland, grant no. 2011/01/B/ST5/06051 to M.E.P.B. L.E. thanks the Robert A. Welch Foundation for an endowed chair, grant no. AH-0033, and the US NSF, grants CHE-1110967 and CHE-1124075. Acknowledgement is made to the OLYMPUS company for the Microscope LEXT OLS4000 measurements. SEM and TEM, IR, Raman, and spectrofluorimeter instruments were funded by the European Funds for Regional Development and the National Funds of Ministry of Science and Higher Education, as part of the Operational Programme Development of Eastern Poland 2007–2013, project: POPW.01.03.00–20–034/09–00.

Keywords: carbon nanomaterials · composites · flavonoid · nanoparticles · polymers · quercetin

[1] a) D. Chen, G. Wang, J. Li, *J. Phys. Chem. C* **2007**, *111*, 2351–2367; b) M. Valcárcel, S. Cardenas, M. Simonet, *Anal. Chem.* **2007**, *79*, 4788–4797.

[2] a) R. D. Averitt, D. Sarkar, D. Halas, *Phys. Rev. Lett.* **1997**, *78*, 4217–4220; b) H. Gao, Y. Kong, D. Cui, C. S. Ozkan, *Nano Lett.* **2003**, *3*, 471–473; c) C. Dwyer, M. Guthold, M. Falvo, S. Washburn, R. Superfine, D. Erie, *Nanotechnology* **2002**, *13*, 601–604; d) J. Kong, H. Dai, *J. Phys. Chem. A J. Phys. Chem. B.* **2001**, *105*, 2890–2893; e) J. L. Anderson, D. W. Armstrong, G. Wei, *Anal. Chem.* **2006**, *78*, 2892–2902; f) J. S. Wilkes, *Green Chem.* **2002**, *4*, 73–80.

[3] Y. Xiao, F. Patolsky, E. Katz, J. F. Heinfled, I. Willner, *Science* **2003**, *299*, 1877–1.

[4] A. Hirsch, *Fullerenes and Related Structures* **1999**, *199*, 1–65.

[5] A. Palkar, F. Melin, C. M. Cardona, B. Elliott, A. K. Naskar, D. D. Edie, A. Kumbhar, L. Echegoyen, *Chem. Asian J.* **2007**, *2*, 625–633.

[6] Y. Liu, R. L. Wal Vander, V. N. Khabashesku, *Chem. Mater.* **2007**, *19*, 778–786.

[7] Y. Y. Yang, S. W. Chen, Q. B. Xue, A. Biris, W. Zhao, *Electrochim. Acta* **2005**, *50*, 3061–3067.

[8] C. T. Cioffi, A. Palkar, F. Melin, A. Kumbhar, L. Echegoyen, M. Melle-Franco, F. Zerbetto, G. M. Aminur Rahman, Ch. Ehli, V. Sgobba, D. M. Guldi, M. Prato, *Chem. Eur. J.* **2009**, *15*, 4419–4427.

[9] L. Zhou, Ch. Gao, D. Zhu, W. Xu, F. F. Chen, A. Palkar, L. Echegoyen, E. S-W. Kong, *Chem. Eur. J.* **2009**, *15*, 1389–139.

[10] M. E. Plonska-Brzezinska, J. Mazurczyk, J. Breczko, B. Palys, A. Lapinski, L. Echegoyen, *Chem. Eur. J.* **2012**, *18*, 2600–2608.

[11] M. E. Plonska-Brzezinska, J. Breczko, B. Palys, L. Echegoyen, *ChemPhysChem*, **2013**, *14*, 116–124.

[12] M. E. Plonska-Brzezinska, M. Lewandowski, M. Błaszyk, A. Molina-Ontoria, T. Luciński, L. Echegoyen, *ChemPhysChem*, **2012**, *13*, 4134–4141.
[13] J. Breczko, K. Winkler, M. E. Plonska-Brzezinska, A. Villalta-Cerdas, L. Echegoyen, *J. Mater. Chem.* **2010**, *20*, 7761–7768.
[14] J. Breczko, M. E. Plonska-Brzezinska, L. Echegoyen, *Electrochim. Acta* **2012**, *72*, 61–67.
[15] J. Luszczyn, M. E. Plonska-Brzezinska, A. Palkar, A. T. Dubis, A. Simionescu, D. T. Simionescu, B. Kalska-Szostko, K. Winkler, L. Echegoyen, *Chem. Eur. J.* **2010**, *16*, 4870–4880.
[16] J. C. Isenburg, D. T. Simionescu, N. R. Vyavahare, *Biomaterials* **2004**, *25*, 3293–3302.
[17] M. Hamburger, K. Hostettmann, *Phytochemistry* **1991**, *30*, 3864–3874.
[18] M. Tomczyk, K. P. Latté, *J. Ethnopharmacol.* **2009**, *122*, 184–204.
[19] H. Lei, J. Luo, L. Tong, L.-Q. Peng, Y. Qi, Z.-G. Jia, Q. Wei, *Food Chem.* **2011**, *127*, 1169–1174.
[20] H. J. Lucas, C. M. Brauch, L. Settas, T. C. Theoharides, *Int. J. Immunopathol. Pharmacol.* **2006**, *19*, 5–10.
[21] J. J. Hilliard, H. M. Krause, J. I. Bernstein, J. A. Fernandez, V. Nguyen, K. A. Ohemeng, J. F. Barrett, *Adv. Exp. Med. Biol.* **1995**, *390*, 59–69.
[22] a) O. Shenderova, T. Tyler, G. Cunningham, M. Ray, J. Walsh, M. Casulli, S. Hens, G. McGuire, V. Kuznetsov, S. Lipa, *Diamond Relat. Mater.* **2007**, *16*, 1213–1217; b) A. S. Rettenbacher, M. W. Perpall, L. Echegoyen, J. Hudson, D. W. Smith, Jr. , *Chem. Mater.* **2007**, *19*, 1411–1417; c) L. Zhou, Ch. Gao, D. Zhu, W. Xu, F. F. Chen, A. Palkar, L. Echegoyen, E. S.-W. Kong, *Chem. Mater.* **2009**, *21*, 1389–1396; d) A. S. Rettenbacher, B. Elliott, J. S. Hudson, A. Amirkhanian, L. Echgeoyen, *Chem. Eur. J.* **2006**, *12*, 376–387.
[23] a) H. C. Wang, Y. Li, M. J. Yang, *Sensors and Actuators B* **2007**, *124*, 360–367; b) S. Qin, D. Qin, W. T. Ford, J. E. Herrera, D. E. Resasco, *Macromolecules* **2004**, *37*, 9963–9967.
[24] a) L. Feng, J. Zheng, H. Yang, Y. Guo, W. Li, X. Li, *Solar Energy Mater. Solar Cells* **2011**, *95*, 644–650; b) Y. Liu, Ch. Cao, J. Li, *Electrochim. Acta* **2010**, *55*, 3921–3926; c) A. K. Chakraborty, K. S. Coleman, *J. Nanosci. Nanotechnol.* **2008**, *8*, 4013–4016; d) S. Yesil, G. Bayram, *Polym. Eng. Sci.* **2011**, *51*, 1286–1300.
[25] Y. Koyama, E. Yamada, T. Ito, Y. Mizutani, T. Yamaoka, *Macromol. Biosci.* **2002**, *2*, 251–256.
[26] K.-J. Eichhorn, A. Fahmi, G. Adam, M. Stamm, *J. Mol. Struct.* **2003**, *661*, 161–170.
[27] X.-G. Li, M.-R. Huang, W. Duan, *Chem. Rev.* **2002**, *102*, 2925–3030.
[28] a) Y. Furukawa, F. Ueda, Y. Ohydo, I. Harada, T. Nakajima, T. Kawagoe, *Macromolecules* **1988**, *21*, 1297–1305; b) S. Quillard, G. Louarn, S. Lefrant, A. G. MacDiarmid, *Phys. Rev. B* **1994**, *50*, 12496–12508.
[29] J. Chen, M. A. Hamon, H. Hu, Y. Chen, A. M. Rao, P. C. Eklund, R. C. Haddon, *Science* **1998**, *282*, 95–98.
[30] a) F. Tuinstra, J. L. Koenig, *J. Chem. Phys.* **1970**, *53*, 1126–1130; b) R. Al-Jishi, G. Dresselhaus, *Phys. Rev. B* **1982**, *26*, 4514–4522.
[31] R. L. Brinkley, R. B. Gupta, *Ind. Eng. Chem. Res.* **1998**, *37*, 4823–4827.
[32] a) A. Star, D. W. Steuerman, J. R. Heath, J. R. Stoddart, *Angew. Chem.* **2002**, *114*, 2618–2622; *Angew. Chem. Int. Ed.* **2002**, *41*, 2508–2512; b) P. Bonnet, M. Gresil, H. Bizot, I. Riou, P. Bertoncini, A. Buelon, O. Chauvet, *J. Nanopart. Res.* **2010**, *12*, 545–550.
[33] a) E. Falkovskaia, P. K. Sengupta, M. Kasha, *Chem. Phys. Lett.* **1998**, *297*, 109–114; b) J. Guharay, B. Sengupta, P. K. Sengupta, *Proteins: Structure Function and Genetics* **2001**, *43*, 75–81.
[34] a) D. S. Knight, W. B. White, *J. Mater. Res.* **1989**, *4*, 385–393; b) R. J. Nemanich, S. A. Solin, *Phys. Rev. B* **1979**, *20*, 392–401.
[35] a) J. E. Pereira da Silva, S. I. Cordoba de Torresi, D. L. A. de Fria, M. L. A. Temperini, *Synth. Met.* **1999**, *101*, 834–835; b) M. Cochet, W. K. Maser, A. M. Benito, A. Callejas, M. T. Martinez, J. M. Benoit, J. Schreiberb, O. Chauvet, *Chem. Commun.* **2001**, 1450–1451; c) A. Star, J. F. Stoddart, D. Steuerman, M. Diehl, A. Bouaki, E. W. Wong, X. Yang, S. W. Chung, H. Choi, J. R. Heath, *Angew. Chem.* **2001**, *113*, 1771–1775; *Angew. Chem. Int. Ed.* **2001**, *40*, 1721–1725; d) S. Quillard, M. I. Boyer, M. Cochet, J.-P. Buisson, G. Louran, S. Lefrant, *Synth. Met.* **1999**, *101*, 768–771; e) D. E. Stilwell, S. M. Park, *J. Electrochem. Soc.* **1988**, *135*, 2491–2496; f) D. E. Stilwell, S. M. Park, *J. Electrochem. Soc.* **1988**, *135*, 2254–2262; g) Y. Wei, W. W. Focke, G. E. Wnek, A. Ray, A. G. Macdiarmid, *J. Phys. Chem.* **1989**, *93*, 495–499.
[36] a) A. C. Gutierrez, M. H. Gehlen, *Spectrochim. Acta Part A* **2002**, *58*, 83–89; b) B. Sengupta, P. K. Sengupta, *Biochem. Biophys. Res. Commun.* **2002**, *299*, 400–403.
[37] V. L. Kuznetsov, A. L. Chuvilin, Y. V. Butenko, I. Y. Malkov, V. M. Titov, *Chem. Phys. Lett.* **1994**, *222*, 343–351.
[38] A. T. Rodriguez, M. Chen, Z. Chen, C. J. Brinker, H. Fan, *J. Am. Chem. Soc.* **2006**, *128*, 9276–9277.

Received: January 2, 2013
Published online: March 6, 2013

